NIH Public Access
Author Manuscript
Biomaterials. Author manuscript; available in PMC 2010 November 1.

Published in final edited form as:
Biomaterials. 2009 November ; 30(32): 6426–6434. doi:10.1016/j.biomaterials.2009.08.012.

Partially Nanofibrous Architecture of 3D Tissue Engineering Scaffolds

Guobao Wei[1] and **Peter X Ma**[1,2,3,*]

[1]Department of Biomedical Engineering, University of Michigan, Ann Arbor, MI 48109-2209, USA

[2]Department of Biologic and Materials Sciences, University of Michigan, Ann Arbor, MI 48109-1078, USA

[3]Macromolecular Science and Engineering Center, University of Michigan, Ann Arbor, MI 48109-1055, USA

Abstract

An ideal tissue-engineering scaffold should provide suitable pores and appropriate pore surface to induce desired cellular activities and to guide 3D tissue regeneration. In the present work, we have developed macroporous polymer scaffolds with varying pore wall architectures from smooth (solid), microporous, partially nanofibrous, to entirely nanofibrous ones. All scaffolds are designed to have well-controlled interconnected macropores, resulting from leaching sugar sphere template. We examine the effects of material composition, solvent, and phase separation temperature on the pore surface architecture of 3D scaffolds. In particular, phase separation of PLLA/PDLLA or PLLA/PLGA blends leads to partially nanofibrous scaffolds, in which PLLA forms nanofibers and PDLLA or PLGA forms the smooth (solid) surfaces on macropore walls, respectively. Specific surface areas are measured for scaffolds with similar macroporosity but different macropore wall architectures. It is found that the pore wall architecture predominates the total surface area of the scaffolds. The surface area of a partially nanofibrous scaffold increases linearly with the PLLA content in the polymer blend. The amounts of adsorbed proteins from serum increase with the surface area of the scaffolds. These macroporous scaffolds with adjustable pore wall surface architectures may provide a platform for investigating the cellular responses to pore surface architecture, and provide us with a powerful tool to develop superior scaffolds for various tissue engineering applications.

Keywords

scaffold; biomaterials; tissue regeneration; polymers; nanofiber

Introduction

In tissue engineering, scaffolds are used to promote tissue regeneration by providing appropriate pores and pore wall surface to foster and direct cellular attachment, migration, proliferation, desired differentiation, tissue regeneration and organization in three dimensions

© 2009 Elsevier Ltd. All rights reserved.

*Corresponding author: Peter X. Ma, PhD, Professor, 1011 North University Ave., Room 2211, Department of Biologic and Materials Sciences, University of Michigan, Ann Arbor, MI 48109-1078, Tel: (734) 764-2209, Fax: (734) 647-2110, mapx@umich.edu

Publisher's Disclaimer: This is a PDF file of an unedited manuscript that has been accepted for publication. As a service to our customers we are providing this early version of the manuscript. The manuscript will undergo copyediting, typesetting, and review of the resulting proof before it is published in its final citable form. Please note that during the production process errors may be discovered which could affect the content, and all legal disclaimers that apply to the journal pertain.

NIH-PA Author Manuscript
NIH-PA Author Manuscript
NIH-PA Author Manuscript

NIH-PA Author Manuscript

NIH-PA Author Manuscript

NIH-PA Author Manuscript

(3D) [1-6]. Recent studies indicate certain parameters to be critical in scaffold design, in which the 3D pores are essential [2,6,7]. The porous features include 3D macroporosity, interconnected microporosity and micro-/nano-scaled surface architectures [8]. The hierarchical porous structures of the scaffolds affect not only the mechanical and degradation properties, but also the biological function of the cells and the tissue regeneration [9-12].

Extracellular matrix (ECM) molecules have been used as tissue culture substrates for a long time and provide a good framework for synthetic scaffold design and fabrication. Despite the complexity of ECM structures due to the involvement of various biomacromolecules and the different ways by which they are organized, an important common feature of native ECM is the nanoscaled dimensions of their physical structures [13]. For example, collagen (type I) is the major organic component of bone ECM and is organized in fibrillar bundles with a diameter range of 50 to 500 nanometers. Notably, the nanoscaled fibrillar structure of collagen has been demonstrated to be critical to cellular activities [14,15]. The nanofibrous architecture of a synthetic polymer scaffold, which mimics the nanofibrous structure of collagen, has been shown to profoundly affect the biological activity of cells [10,11]. It is now recognized that nano-sized surface architectures are critical to cell function and tissue regeneration [12,16]. Previously, we developed a combined porogen template leaching and phase separation technique for 3D scaffold fabrication [3,8]. In such a technique, porogen template was utilized to control 3D macroporosity and interpore connectivity while phase separation process was manipulated to generate different pore wall surface architectures. It has also been demonstrated that synthetic polymer nanofibers possess certain properties that are comparable to natural collagen nanofibers [9-11]. These nano-fibrous materials adsorb increased levels of attachment proteins (fibronectin, vitronectin and laminin) compared to smooth materials and increase expression of integrins that are active in cellular attachment to these proteins [9,17,18]. The nanofibers also affect cellular morphology of both embryonic stem cells [17,18] and committed cells [12]. On nanofibers, cells assumed a morphology that more closely resemble in vivo morphology [12] that promote osteoblastic differentiation and mineralized tissue regeneration both in vitro and in vivo [19,20].

To further understand how nano architectures affect cell-material interactions in a 3D environment and to develop optimal scaffolds for the regeneration of various tissues, we have to develop techniques that are capable of generating scaffolds with varying surface architectures to systematically study their biological effects. One major challenge is the difficulty in controlling the surface architecture of pores in the scaffolds. Few studies have been able to investigate the effect of surface architectures on cellular activity in a 3D porous scaffold [11,21]. In this work, we aimed to develop techniques to manipulate the surface architecture to enable such investigations and the development of optimal scaffolds for tissue engineering.

Materials and Methods

Poly(L-lactic acid) (PLLA) (RESOMER® L207, $\eta_{i.v.}$=1.6 dl/g) and poly(DL-lactic acid) (PDLLA) (RESOMER® R208, $\eta_{i.v.}$=1.7 dl/g) were purchased from Boehringer Ingelheim (Ingelheim, Germany) and used as received. Poly(lactic-*co*-glycolic acid) (PLGA50-47K, Medisorb®, LA:GA=50:50, Mw=47 kDa) was obtained from Alkermes Inc. (Wilmington, OH). D-fructose (m.p. 119-122°C), mineral oil, and sorbitanmonooleate (Span 80) were from Sigma (St. Louis, MO). Cyclohexane and hexane were from Fisher Scientific (Pittsburgh, PA). Tetrahydrofuran (THF), 1,4-dioxane, dichloromethane (DCM) and all other chemicals were from Aldrich Chemical Company (Milwaukee, WI).

NIH-PA Author Manuscript

NIH-PA Author Manuscript

NIH-PA Author Manuscript

2D Film preparation

Polymer blends of PLLA and PDLLA or PLGA with varying ratios were dissolved in THF at 60°C to form a homogenous solution with a concentration of 10% (wt/v%). The polymer solution was then cast into a lumen between two glass plates (space thickness around 100 μm created by sticky tapes). The glass plates containing the polymer solution were placed in a -20° C refrigerator, phase separated for 2 hours, and then immersed into ice-cold distilled water to exchange THF. Distilled water was changed 4 times over a time period of 24 hours. Polymer films were easily removed from glass plates after the completion of solvent exchange and were freeze-dried for 3 days to remove the water and residual solvent.

3D Scaffold fabrication

Macroporous scaffolds were fabricated by a combined phase separation and sugar sphere template leaching technique [8]. Briefly, 0.6-0.8 ml of 10 wt% polymer solution in THF was cast into an assembled sugar template (formed from bound sugar spheres 250-425 μm in diameter and heat treated at 37°C for 20 minutes) under mild vacuum. The polymer solution in the sugar template was phase separated by lowering the temperature and then the constructs were immersed in cyclohexane to exchange solvent for 2 days. After freeze-drying, the sugar sphere template was leached away in distilled water and the highly porous polymer scaffold was freeze-dried. Scaffolds with different macropore surface architectures were prepared under different processing conditions: (i) polymer blends of PLLA/PDLLA with varying weight ratios (100:0, 75:25, 50:50, 25:75, 15:85 and 0:100) and PLLA/PLGA (PLLA:PLGA =75:25) were phase separated in THF at -20°C; (ii) PLLA was phase separated in dioxane at two different temperatures, in liquid nitrogen (at -196°C) and at -20°C, respectively; (iii) PLLA in a solvent mixture (THF/dioxane) with varying volume ratios (100:0, 60:40, 40:60, 20:80 and 0:100) was phase separated in liquid nitrogen (-196°C). Solid-walled PLLA scaffolds were also fabricated using solvent (dichloromethane) evaporation and sugar sphere template leaching techniques as the control scaffolds for the partially or totally nanofibrous scaffolds in this study.

Morphological characterization

The surface morphologies of films and macroporous scaffolds were examined using scanning electron microscopy (SEM) (Philips XL30 FEG) at 15 KV. Before SEM examination, the samples were cut with a razor blade or fractured after liquid nitrogen treatment and coated with gold for 120 s using a sputter coater (Desk-II, Denton Vacuum Inc.).

Surface area measurement

The specific surface area (A_{BET}) of the polymer scaffolds was measured using a BELSORP-mini apparatus (BEL Japan, Inc.). Adsorption/desorption isotherms of samples were obtained using nitrogen as the adsorbate and liquid nitrogen as the cooling medium. The surface areas of the polymer scaffolds were calculated from Brunauer-Emmett-Teller (BET) plot of adsorption/desorption isotherm using adsorption points in the P/P_0 range of 0.1-0.3 (BELSORP-mini analysis software).

Protein adsorption

Protein adsorption was performed by incubating polymer scaffolds in a phosphate buffered saline (PBS, 0.1M, pH=7.4) containing 20% fetal bovine serum (FBS). Three disk-shaped specimens with dimensions of 7.2 mm in diameter and 2 mm in thickness were used for each group. Before incubation of the scaffolds in the medium (containing proteins), samples were prewetted in 70% ethanol for 30 minutes and then rinsed with PBS three times overnight under gentle shaking. Samples were then put in a 24-well culture plate (one sample in each well) and 1.5 ml FBS/PBS solution was added into each well. The scaffolds were incubated at 37°C for

NIH-PA Author Manuscript

NIH-PA Author Manuscript

NIH-PA Author Manuscript

12 hours. The amounts of adsorbed proteins on the scaffolds (μg/mg scaffold) were quantified using a commercial protein assay kit, microBCA (Pierce, Rockford, IL), using bovine serum albumin (BSA) as the standard [9].

Results

Partially nanofibrous films

Partially nanofibrous "2D" films were obtained from PLLA/PDLLA polymer blends with varying weight ratios. Figure 1 shows the surface architectures of PLLA/PDLLA partially nanofibrous films fabricated using a thermally induced phase separation technique. By lowering the temperature to -20°C, phase separation was initiated between the solvent (THF) and the polymer blend, which led to a highly microporous film. Phase separation also happened between the two polymers, i.e., PLLA and PDLLA, possibly due to their differences in crystallinity and solubility. The presence of PDLLA seems not to significantly affect the formation of PLLA nanofibrous network. The nanofibrous domains increase with the amount of PLLA, while the smooth pore surface domains increase with the amount of PDLLA in the polymer blend. The results suggest that the PDLLA contributes to smooth (solid) surface architecture while the PLLA contributes to nanofibrous architecture within the film. At a high proportion of PDLLA in the blend, however, PLLA nano-fibers become embedded in PDLLA domains to form a denser film. The microporosity of the film decreases with the increase of PDLLA/PLLA ratio.

Macroporous Partially Nanofibrous Scaffolds

Partially nanofibrous PLLA/PDLLA scaffolds—PLLA/PDLLA polymer blends were also fabricated into 3D macroporous scaffolds. Figure 2 shows the surface morphologies of macropores in the partially nanofibrous PLLA/PDLLA scaffolds, which were phase separated in THF at -20°C. In agreement with the partially nanofibrous PLLA/PDLLA 2D films, the PLLA/PDLLA blend scaffolds exhibited partially nanofibrous architecture, which resulted from the phase separations of two different polymers. The phase separation of crystalline PLLA in THF resulted in nanofibrous architectures on the macropore walls while the phase separation of amorphous PDLLA resulted in solid-walled (smooth) pore surface domains under the same conditions. With low proportions of PDLLA (<50%), PDLLA domains (in diameter of about 10 μm) were distributed uniformly but sparsely throughout the nanofibrous PLLA network. With the increase of PDLLA portion in the polymer blend, PDLLA domains extended and connected to each other. At high ratios of PDLLA (>50%), a continuous porous PDLLA film was formed to cover the PLLA nanofibers on the inner surfaces of the macropores. Pure PLLA scaffold (100% PLLA) exhibited only continuous nanofibrous network on the macropore walls (Figure 2 A&B) while the pure PDLLA scaffolds (100% PDLLA) exhibited only non-fibrous smooth pore surfaces (Figure 2 K&L). With various ratios of PLLA/PDLLA, both nanofibers and smooth domains were found on the macropores of the highly porous polymer blend scaffolds (Figure 2 C-J). The smooth PDLLA domains were found more abundant on the pore surfaces of the macropore walls, under which nanofibrous PLLA network distributed uniformly and throughout (Figure 2 M).

Partially nanofibrous PLLA/PLGA scaffolds—When PLGA was used to replace PDLLA in the polymer blend, pore surfaces of nanofibrous and smooth domains were also obtained in the highly porous PLLA/PLGA scaffolds (Figure 3).

PLLA scaffolds with microporous walls—Figure 4 demonstrates the effect of phase separation conditions (solvent and temperature) on pore structures of the scaffolds. Since the macroporosity was generated by sugar sphere template leaching technique, phase separation did not affect the macroporosity and interpore connectivity of the scaffolds. However, the phase

NIH-PA Author Manuscript

NIH-PA Author Manuscript

NIH-PA Author Manuscript

separation solvent and temperature affected the micro/nano-structures significantly. When PLLA was phase separated in dioxane instead of THF, scaffolds were microporous instead of nano-fibrous in terms of pore wall architecture. When PLLA was phase separated in dioxane at -20°C, no nanofibers were obtained. Instead, well-connected micropores (in order of ten microns) were present throughout the macropores (250-425 μm) (Figure 4 A&B). By lowering the phase separation temperature to -196°C (liquid nitrogen), typical ladder-like microporous structures were observed on macropore walls and the micropores were smaller and more regular than those phase separated at -20°C.

PLLA scaffolds with microporous and nanofibrous pore walls—Figure 5 shows the effect of solvent mixture on the architecture of pore walls in a 3D scaffold. Phase separation of PLLA in THF at -196°C (liquid nitrogen) resulted in continuous nanofibrous network on macropore walls, which is similar to that phase separated at -20°C (Figure 5 A-C and Figure 2 A&B). The diameter of nanofibers was 50-500 nm and the average unit length (the length of the fiber between two junctions) was a few microns. The distance between nanofibers was in the order of 1 micron. With the addition of dioxane into THF, the dimensions of PLLA nanofibers (diameter, length, and distance between them) decreased significantly. The individual fibers became smaller in diameter but more bundled together. In addition, ladder-like porous structures appeared on the nanofibrous macropore walls. The ladder-like pore structure is typically associated with the solid-liquid phase separation of a PLLA/dioxane solution [22]. The increase of dioxane in the solvent mixture led to denser PLLA nanofibrous networks and more ladder-like microporous structures on the macropore walls (Figure 5 D-L).

Surface Area

The surface areas of scaffolds can be significantly different when their pore surface morphologies are different. The pure nanofibrous PLLA scaffolds have a very high surface area of around 110 m^2/g, which is thousands of times higher than that of pure solid-walled PDLLA scaffolds (<0.1 m^2/g, below which is too low to be measurable using the BELSORP-mini surface area analyzer). In PLLA/PDLLA blend scaffolds, the surface area increases linearly with the increase of PLLA content (Figure 6 A). Since all scaffolds have similar macroporous structures, the substantial difference in surface area is mainly due to the difference in the amount of PLLA nanofibers resulted from PLLA phase separation. Macroporosity generated from sugar sphere template contributes little to the total surface area, as the PDLLA scaffold has a very low surface area (<0.1 m^2/g). PLLA scaffolds prepared using different solvents and/or temperatures have very different surface morphologies of the macropores, which result in significantly different surface areas (Figure 6 B). Compared to nanofibrous PLLA scaffolds, the PLLA scaffolds with microporous walls have significantly lower surface areas, 4.13 and 0.89 m^2/g for phase separation in dioxane at -196°C and -20°C, respectively. However, PLLA scaffolds generated from phase separation in dioxane (with micropores) show much higher surface areas than solid-walled PLLA or PDLLA scaffolds (prepared through dichloromethane evaporation). PLLA scaffolds generated from phase separation in THF/dioxane solvent mixture show higher surface areas than those phase separated in THF or dioxane alone (Figure 6C). This is likely due to the denser and smaller nanofibers presented in the PLLA scaffolds that were phase separated in the THF/dioxane mixture. However, the smaller diameter of the nanofibers seems counterbalanced by the fiber bundling effect, resulting in a less dramatic increase in the total surface area.

Protein Adsorption

The large surface area of nanofibrous scaffold contributed to the high protein adsorption capacity. PLLA scaffolds with nanofibrous textures adsorbed about 8 times greater amounts of serum proteins than those with smooth (solid-walled) pore surfaces (Figure 7 A). Micropore-walled scaffolds adsorbed more protein than solid-walled scaffolds. The protein adsorption

NIH-PA Author Manuscript

NIH-PA Author Manuscript

NIH-PA Author Manuscript

capacity is correlated well with the total surface area of the scaffold. The higher surface area results in more protein adsorption. In the partially nanofibrous PLLA/PDLLA scaffolds, the amount of protein adsorption on the scaffold increased with the increase of PLLA content in the polymer blend likely because of the higher surface area from the PLLA nanofibers (Figure 7 B). The protein adsorption on the scaffold may contribute to enhanced cell adhesion and tissue regeneration [9]. The nanofibrous architecture and the associated protein adsorption contribute to the cellular differentiation and tissue regeneration potentials [10-12].

Discussion

It is well known that macropores and interconnectivity between them in a scaffold are essential for cell growth, migration, tissue formation and vascularization in tissue engineering [1]. Different cell/tissue types may require different macropore sizes and different degrees of interconnectivity [23,24]. The interactions between cells and biomaterials occur at the interface, i.e. on the pore walls of the 3D scaffold. Surface morphology or topography is therefore important [7,13]. Manipulation of surface topography on the macropore walls can significantly affect cell-scaffold interactions and therefore tissue formation and function [9, 10]. Techniques such as surface etching and micro-/nano-fabrication have been utilized to achieve spatial, topographical, and chemical patterns to control cells. However, previous work has been focused on 2D substrates [25,26]. Design of surface architectures in a 3D porous scaffold and investigation of their effects on cell function remain limited [12].

In this work, we have developed a technique to prepare 3D porous scaffolds with adjustable macropore wall architectures varying from solid-walled (smooth), microporous (with random or ladder-like micropores on the macropores), partially nanofibrous (a mixture of nanofibrous and smooth domains), and totally nanofibrous ones (Figures 2 and 3). Importantly, this technique is able to maintain similar well-interconnected macropores (e.g., 250-425 μm in diameter and 96% porosity) for all scaffolds with different macropore wall architectures. The macroporosity and pore size have been demonstrated to be suitable for osteoblast differentiation and bone regeneration [3,11,27]. In nanofibrous PLLA scaffolds, the fiber characteristics (such as fiber diameter, unit fiber length and fiber density) can be manipulated by controlling the phase separation solvent composition (Figure 5). The new scaffolding technique provides us with the ability to control the porous structures of the scaffold from macro, micro to nano scales, allowing for designing or mimicking various physical characteristics of extracellular matrix to enhance scaffold function [2,11,13,28].

Different cell types show different degrees of adhesion and different rates of proliferation on implants with different surface topographies [29-31]. For example, rough titanium surfaces strongly support osteoblast and fibroblast attachment, but discourage epithelial cell attachment and spreading [29]. On a surface with gradient roughness, osteoblasts show a significantly increased proliferation rate with the increase of surface roughness while fibroblasts show the opposite trend in proliferation rate in relation to surface roughness, i.e., a slower proliferation rate with an increased roughness [31]. These observations were made on 2D surfaces. The investigation on cell responses to 3D surface architectures in porous scaffolds is important for the field of tissue engineering and regenerative medicine [9-11].

The scaffolds developed in the present study provide a platform to enable systematic studies of the cellular response and tissue regeneration in relation to different surface architectures in a 3D environment. The manipulation of the scaffold pore wall architecture will also allow us to develop optimal 3D scaffolds for various regenerative therapies. These porous scaffolds with partially nanofibrous and partially smooth domains may also serve as promising 3D matrices for co-culturing different cells that prefer different surface architectures.

NIH-PA Author Manuscript

NIH-PA Author Manuscript

NIH-PA Author Manuscript

The partially nanofibrous PLLA/PDLLA and PLLA/PLGA scaffolds are particularly interesting because the partially nanofibrous scaffolds were essentially made from two polymers with the same chemical composition (PLLA/PDLLA: with different steoregularities and therefore different crystallinities) or similar chemical compositions (PLLA/PLGA) but showed distinctly different domains of nanofibrous and smooth domain morphologies on the macropore walls. It is interesting to notice that the smooth domains are more abundantly located on the surface of the macropore walls while the PLLA nanofibers are more uniformly distributed throughout the pore walls. During phase separation of PLLA/PDLLA polymer blend in THF within the sugar sphere template, it is possible that PDLLA first phase separates from solvent and form smooth domains that preferentially surround the sugar spheres. Upon further decrease of the temperate, PLLA phase separates and form nanofibers throughout the pore walls. The combination of nanofibrous and smooth domains can be utilized to control surface area, protein adsorption profiles, and cellular interactions. The combination of other nanofiber-forming and non-nanofiber-forming polymers may also be able to generate partially nanofibrous and partially smooth domains of films or 3D materials.

Conclusions

Thin porous films and three-dimensional macroporous polymer scaffolds with varying pore wall architectures have been prepared from polymer blends using sugar sphere template leaching and phase separation techniques. The macropore wall architectures of the scaffolds are controlled by the composition of polymer materials, the solvent, and the phase separation temperature. Partially nanofibrous and partially smooth domained thin films and 3D scaffolds were obtained through the phase separation of PLLA/PDLLA and PLLA/PLGA blends. The ratio of polymers in the blend is critical to controlling the ratio of the nanofibrous and the smooth domains in the thin matrix and the 3D scaffold, the total surface area of the scaffold, and the protein adsorption capability. The scaffolds with controlled macropores and manipulable pore wall architectures may serve as a new scaffolding platform technology to direct cell-scaffold interactions and guide 3D tissue regeneration.

Acknowledgements

The authors would like to acknowledge the financial support from the National Institutes of Health (Research Grants DE015384, GM075840 and DE017689: PXM).

References

[1]. Ma, PX. Tissue Engineering. In: Kroschwitz, JI., editor. Encyclopedia of Polymer Science and Technology. Vol. Third ed.. John Wiley & Sons, Inc.; Hoboken, NJ: 2005. p. 261-291.

[2]. Ma PX. Scaffolds for tissue fabrication. Materials Today 2004;7(5):30–40.

[3]. Chen VJ, Ma PX. Nano-fibrous poly(L-lactic acid) scaffolds with interconnected spherical macropores. Biomaterials 2004;25(11):2065–2073. [PubMed: 14741621]

[4]. Ma PX, Zhang RY. Microtubular architecture of biodegradable polymer scaffolds. J Biomed Mater Res 2001;56:469–477. [PubMed: 11400124]

[5]. Muschler GF, Nakamoto C, Griffith LG. Engineering principles of clinical cell-based tissue engineering. J Bone Joint Surg Am 2004;86-A(7):1541–1558. [PubMed: 15252108]

[6]. Cancedda R, Mastrogiacomo M, Bianchi G, Derubeis A, Muraglia A, Quarto R. Bone marrow stromal cells and their use in regenerating bone. Novartis Found Symp 2003;249:133–143. [PubMed: 12708654]discussion 143-137, 170-134, 239-141

[7]. Ma PX. Biomimetic materials for tissue engineering. Advanced Drug Delivery Reviews 2008;60(2): 184–198. [PubMed: 18045729]

[8]. Wei GB, Ma PX. Macro-porous and nano-fibrous polymer scaffolds and polymer/bone-like apatite composite scaffolds generated by sugar spheres. J Biomed Mater Res 2006;78:306–315.

NIH-PA Author Manuscript

NIH-PA Author Manuscript

NIH-PA Author Manuscript

[9]. Woo KM, Chen VJ, Ma PX. Nano-fibrous scaffolding architecture selectively enhances protein adsorption contributing to cell attachment. J Biomed Mater Res 2003;67A(2):531–537.

[10]. Woo KM, Jun JH, Chen VJ, Seo JY, Baek JH, Ryoo HM, et al. Nano-fibrous scaffolding promotes osteoblast differentiation and biomineralization. Biomaterials 2007;28(2):335–343. [PubMed: 16854461]

[11]. Chen VJ, Smith LA, Ma PX. Bone regeneration on computer-designed nano-fibrous scaffolds. Biomaterials 2006;27(21):3973–3979. [PubMed: 16564086]

[12]. Hu J, Liu X, Ma PX. Induction of osteoblast differentiation phenotype on poly(L-lactic acid) nanofibrous matrix. Biomaterials 2008;29(28):3815–3821. [PubMed: 18617260]

[13]. Wei G, Ma PX. Nanostructured Biomaterials for Regeneration. Advanced Functional Materials 2008;18(22):3568–3582.

[14]. Grinnell F, Bennett MH. Ultrastructural studies of cell--collagen interactions. Methods Enzymol 1982;82(Pt A):535–544. [PubMed: 7078448]

[15]. Phillips JE, Hutmacher DW, Guldberg RE, Garcia AJ. Mineralization capacity of Runx2/Cbfa1-genetically engineered fibroblasts is scaffold dependent. Biomaterials 2006;27(32):5535–5545. [PubMed: 16857257]

[16]. Rosenberg MD. Cell guidance by alterations in monomolecular films. Science 1963;139:411–412. [PubMed: 13974905]

[17]. Smith LA, Liu X, Hu J, Ma PX. The influence of three-dimensional nanofibrous scaffolds on the osteogenic differentiation of embryonic stem cells. Biomaterials 2009;30(13):2516–2522. [PubMed: 19176243]

[18]. Smith LA, Liu X, Wang P, Hu J, Ma PX. Enhancing Osteogenic Differentiation of Embryonic Stem Cells by Nanofibers. Tissue Engineering 2009;15:1855–1864. [PubMed: 19196152]

[19]. Woo KM, Chen VJ, Jung H-M, Kim T-I, Shin H-I, Baek J-H, et al. Comparative Evaluation of Nanofibrous Scaffolding for Bone Regeneration in Critical-Size Calvarial Defects. Tissue Engineering 2009;15(DOI: 10.1089=ten.tea.2008.0433):DOI: 10.1089=ten.tea.2008.0433 (in press)

[20]. Wang P, Hu J, Ma PX. The engineering of patient-specific, anatomically shaped, digits. Biomaterials 2009;30(14):2735–2740. [PubMed: 19203788]

[21]. Liu X, Smith LA, Wei GB, Won Y, Ma PX. Surface engineering of nano-fibrous poly(L-lactic acid) scaffolds via self-assembly technique for bone tissue engineering. J Biomed Nanotech 2005;1(1): 54–60.

[22]. Zhang RY, Ma PX. Poly(alpha-hydroxyl acids) hydroxyapatite porous composites for bone-tissue engineering. I. Preparation and morphology. J Biomed Mater Res 1999;44:446–455. [PubMed: 10397949]

[23]. Tsuruga E, Takita H, Itoh H, Wakisaka Y, Kuboki Y. Pore size of porous hydroxyapatite as the cell-substratum controls BMP-induced osteogenesis. J Biochem (Tokyo) 1997;121(2):317–324. [PubMed: 9089406]

[24]. Roy TD, Simon JL, Ricci JL, Rekow ED, Thompson VP, Parsons JR. Performance of degradable composite bone repair products made via three-dimensional fabrication techniques. J Biomed Mater Res A 2003;66(2):283–291. [PubMed: 12888998]

[25]. Deutsch J, Motlagh D, Russell B, Desai TA. Fabrication of microtextured membranes for cardiac myocyte attachment and orientation. J Biomed Mater Res (Appl Biomater) 2000;53(3):267–275.

[26]. Flemming RG, Murphy CJ, Abrams GA, Goodman SL, Nealey PF. Effects of synthetic micro- and nano-structured surfaces on cell behavior. Biomaterials 1999;20(6):573–588. [PubMed: 10213360]

[27]. Ma PX, Choi JW. Biodegradable polymer scaffolds with well-defined interconnected spherical pore network. Tissue Eng 2001;7(1):23–33. [PubMed: 11224921]

[28]. Holy CE, Fialkov JA, Davies JE, Shoichet MS. Use of a biomimetic strategy to engineer bone. J Biomed Mater Res A 2003;65(4):447–453. [PubMed: 12761834]

[29]. Chehroudi B, Gould TR, Brunette DM. The role of connective tissue in inhibiting epithial downgrowth on titanium-coated percutaneous implants. J Biomed Mater Res 1992;26(4):493–515. [PubMed: 1601902]

NIH-PA Author Manuscript

NIH-PA Author Manuscript

NIH-PA Author Manuscript

[30]. Washburn NR, Yamada KM, Simon CG, Kennedy SB, Amis E. High-throughput investigation of osteoblast response to polymer crystallinity: influence of nanometer-scale roughness on proliferation. Biomaterials 2004;25:1215–1225. [PubMed: 14643595]

[31]. Kunzler TP, Drobek T, Schuler M, Spencer ND. Systematic study of osteoblast and fibroblast response to roughness by means of surface-morphology gradients. Biomaterials 2007;28:2175–2182. [PubMed: 17275082]

NIH-PA Author Manuscript
NIH-PA Author Manuscript
NIH-PA Author Manuscript

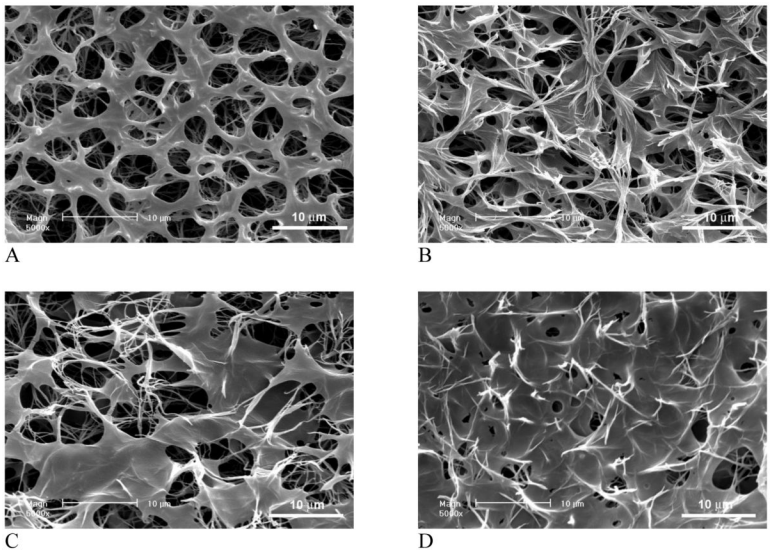

Figure 1.
SEM micrographs of partially nanofibrous PLLA/PDLLA films. (A) PDLLA:PLLA=50:50; (B) PDLLA:PLLA=60:40; (C) PDLLA:PLLA=75:25; (D) PDLLA:PLLA=85:15. The total polymer concentration: 10w/v%. Original magnification: 5,000x.

NIH-PA Author Manuscript
NIH-PA Author Manuscript
NIH-PA Author Manuscript

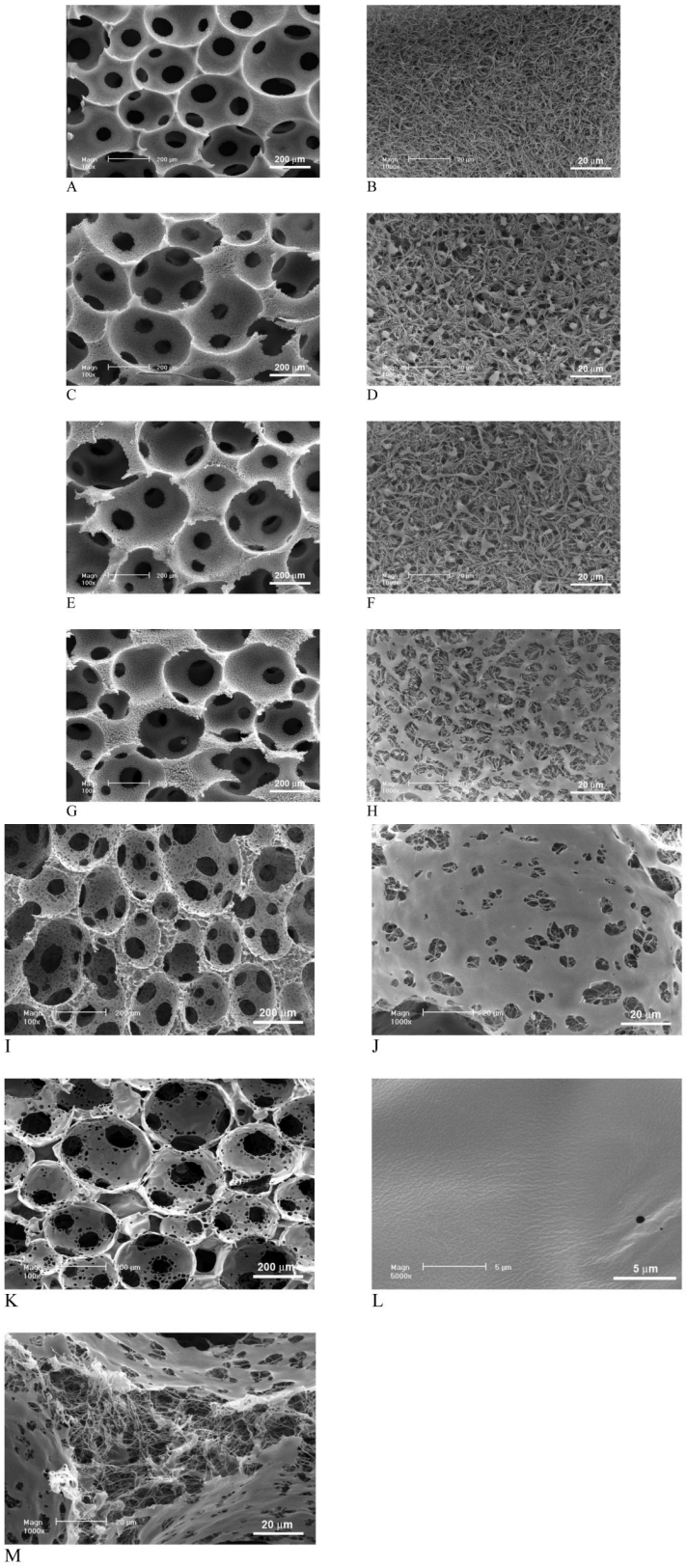

Figure 2.

SEM micrographs of 3D macroporous and partially nanofibrous PLLA/PDLLA scaffolds, phase separated in THF at -20°C. (A,B) 100% PLLA; (C,D) PLLA:PDLLA = 75:25; (E,F) PLLA:PDLLA = 50:50; (G,H) PLLA:PDLLA = 25:75; (I,J,M) PLLA:PDLLA = 15:85; (K,L) 100% PDLLA; (M) Cross section of pore wall to show the distribution of nanofibrous and solid domains (PLLA:PDLLA = 15/85). The total polymer concentration: 10w/v%. Original magnification: 100x for A, C, E, G, I, K; 1,000x for B, D, F, H, J, M; and 5,000x for L.

NIH-PA Author Manuscript
NIH-PA Author Manuscript
NIH-PA Author Manuscript

NIH-PA Author Manuscript

NIH-PA Author Manuscript

NIH-PA Author Manuscript

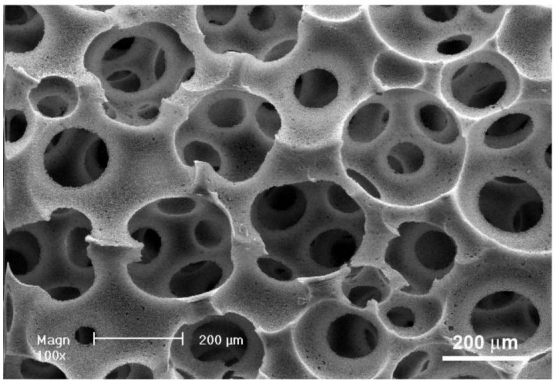

A

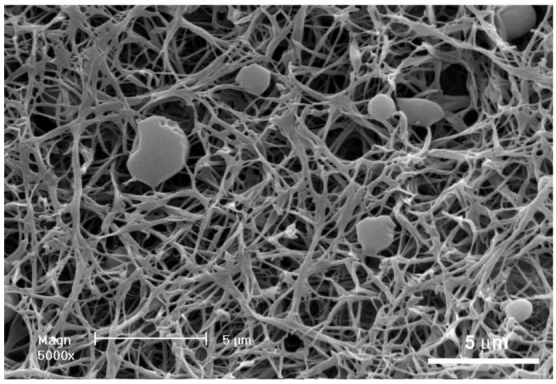

B

Figure 3.

SEM micrographs of macroporous and partially nanofibrous PLLA/PLGA scaffolds, phase separated in THF at -20°C (PLGA:PLLA=25:75). The total polymer concentration was 10w/v%. Original magnification: 100x for A; 5,000x for B.

NIH-PA Author Manuscript

NIH-PA Author Manuscript

NIH-PA Author Manuscript

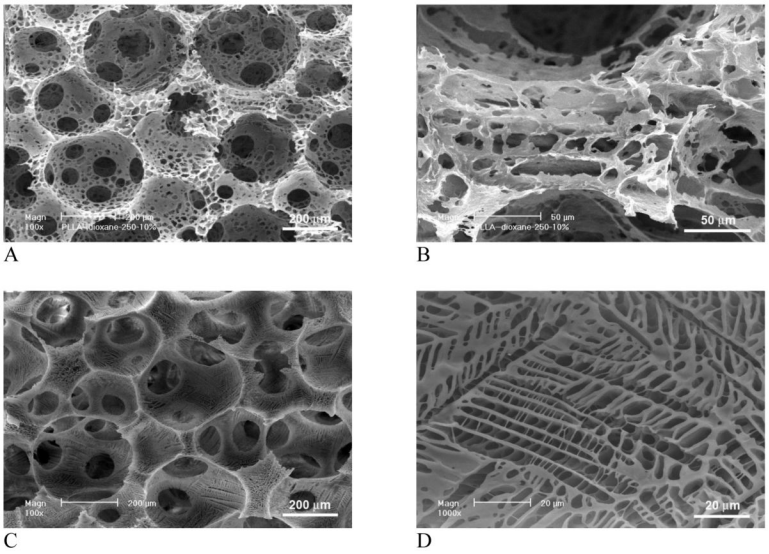

Figure 4.
SEM micrographs of macroporous and microporous PLLA scaffolds, phase separated in dioxane at different temperatures. (A,B) -20°C; (C,D) Liquid nitrogen (-196°C). Original magnification: A & C, 100x; B, 500x; and D, 1,000x.

NIH-PA Author Manuscript

NIH-PA Author Manuscript

NIH-PA Author Manuscript

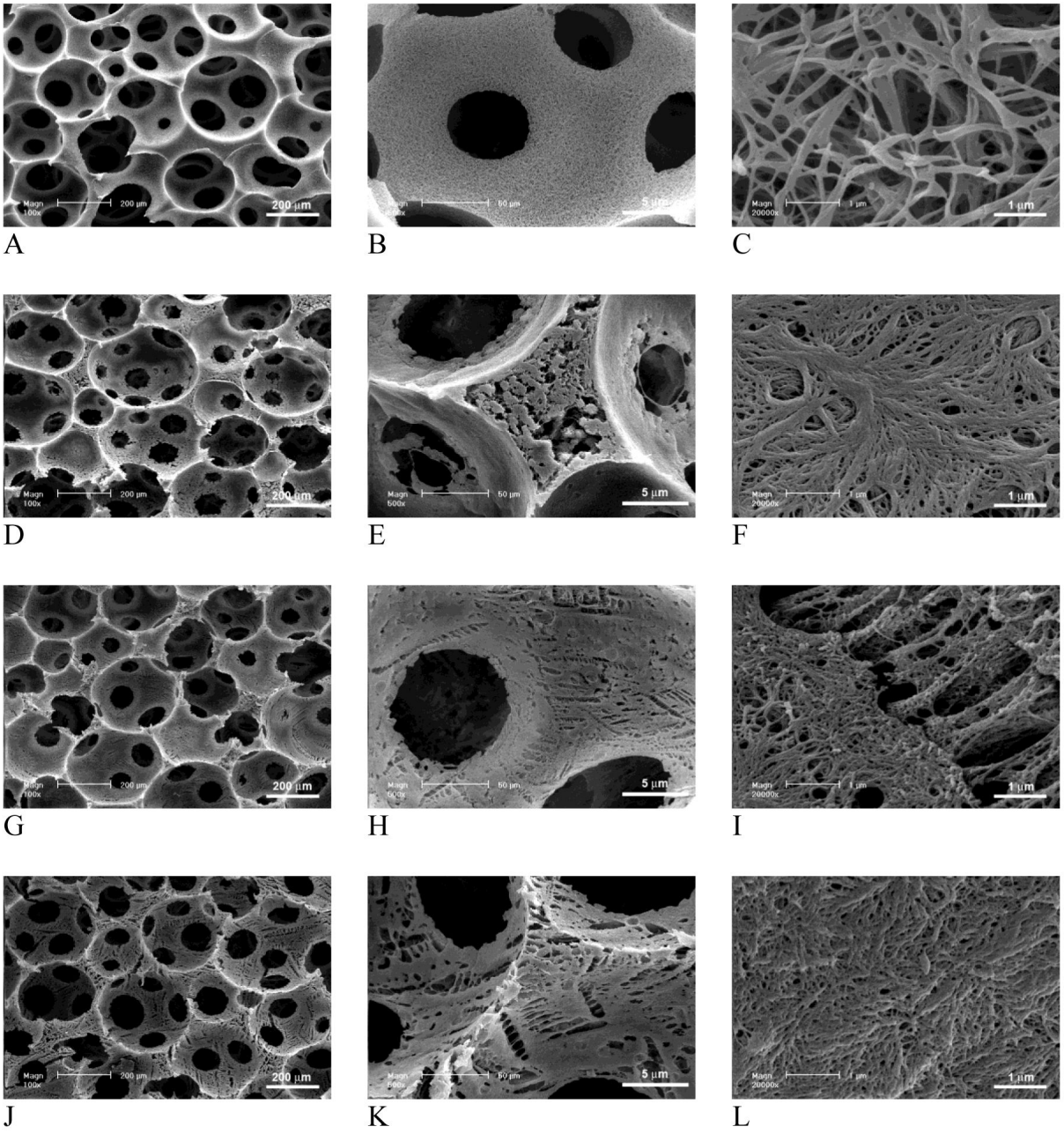

Figure 5.

SEM micrographs of macroporous and nanofibrous PLLA scaffolds, phase separated in dioxane/THF in liquid nitrogen (-196°C). (A-C) THF:dioxane=100:0; (D-F) THF:dioxane=60:40; (G-I) THF:dioxane=40:60; (J-L) THF:dioxane=20:80. Original magnification: 100x for A, D, G, J; 500x for B, E, H, K; and 20,000x for C, F, I, L.

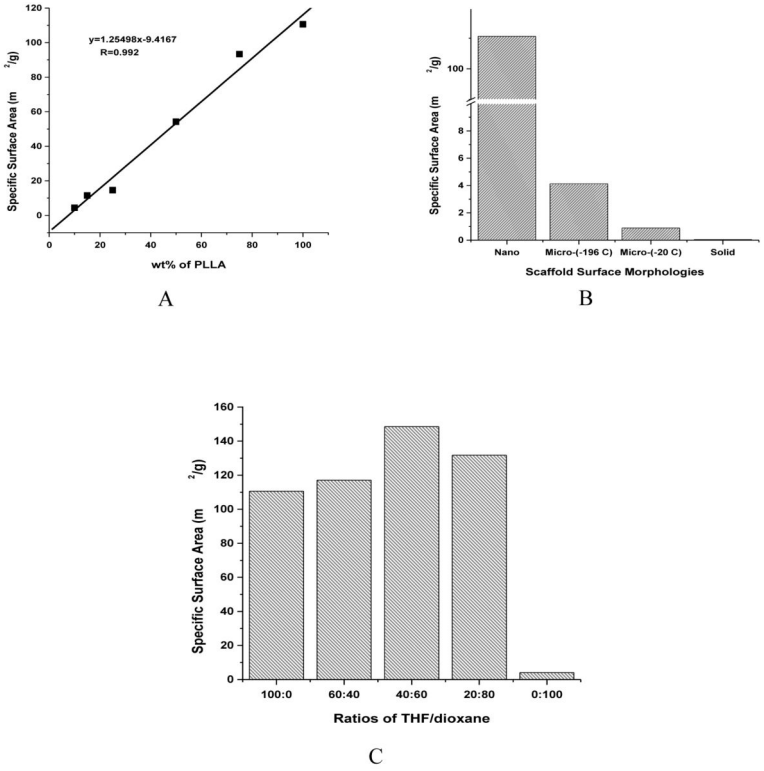

Figure 6.

Specific surface areas of: (A) partially nanofibrous PLLA/PDLLA scaffolds (phase-separated in THF at -20 R°C) as a function of PLLA wt% in the polymer blends; (B) PLLA scaffolds with different pore wall surface morphologies: Nano - nanofibrous, phase separation in THF at -20 C°C; Micro-(-196°C) - microporous, phase separation in dioxane in liquid nitrogen; Micro-(-20°C) - microporous, phase separated in dioxane at -20°C; Solid - solid-walled, generated by solvent evaporation from the polymer solution in dichloromethane; (C) PLLA scaffolds phase separated in the solvent mixture of dioxane/THF with varying ratios, in liquid nitrogen (at -196°C).

NIH-PA Author Manuscript NIH-PA Author Manuscript NIH-PA Author Manuscript

NIH-PA Author Manuscript

NIH-PA Author Manuscript

NIH-PA Author Manuscript

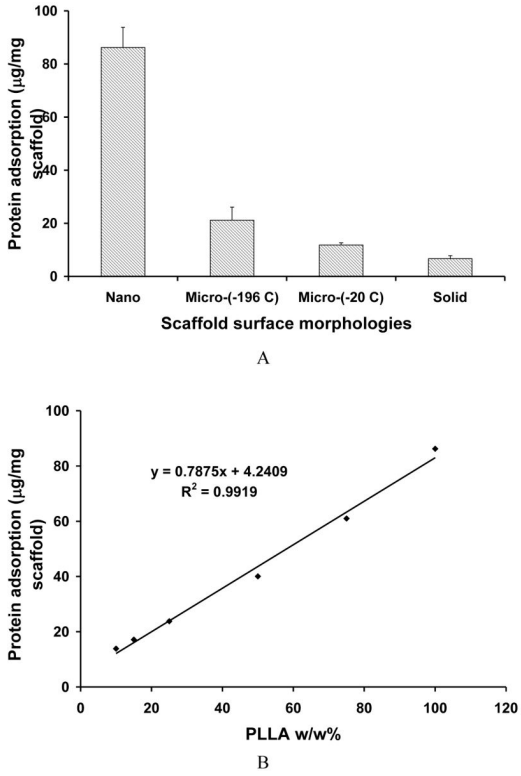

Figure 7.

Serum protein adsorption on macroporous scaffolds with different pore wall surface architectures. (A) PLLA scaffolds phase separated in different solvents: Nano - nanofibrous, phase separated in THF at -20°C; Micro-(-196 C) - microporous, phase separated in dioxane in liquid nitrogen; Micro-(-20°C) - microporous, phase separated in dioxane at -20°C; Solid - solid-walled, generated by solvent evaporation from the polymer solution in dichloromethane; (B) PLLA/PDLLA partially nanofibrous scaffolds with different PLLA wt% in polymer blends, phase-separated in THF at -20°C.